

# Partial Regeneration of the Spent SAPO-34 Catalyst in the Methanol-to-Olefins Process via Steam Gasification

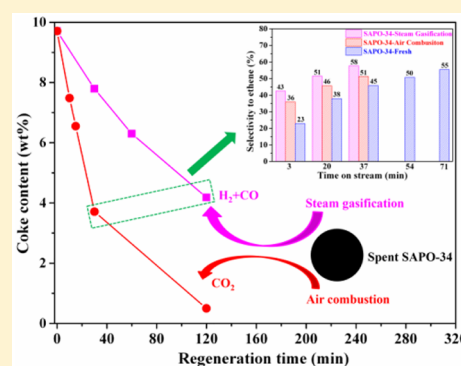
Jibin Zhou,<sup>†,‡</sup> Jinling Zhang,<sup>†</sup> Yuchun Zhi,<sup>†</sup> Jianping Zhao,<sup>†,‡</sup> Tao Zhang,<sup>†</sup> Mao Ye,<sup>\*,†</sup> and Zhongmin Liu<sup>†</sup>

<sup>†</sup>National Engineering Laboratory for Methanol to Olefins, Dalian National Laboratory for Clean Energy, Collaborative Innovation Center of Chemistry for Energy Materials, Dalian Institute of Chemical Physics, Chinese Academy of Sciences, Dalian 116023, P. R. China.

<sup>‡</sup>University of Chinese Academy of Sciences, Beijing 100049, P. R. China

## Supporting Information

**ABSTRACT:** The methanol-to-olefins (MTO) reaction over the SAPO-34 catalyst suffers rapid deactivation due to coke deposition. Here, partial regeneration methods with air combustion and steam gasification were investigated. The results showed that both methods could not only reactivate the spent SAPO-34 catalyst but also prompt ethylene selectivity. Whereas, steam gasification was more effective, by which the initial ethylene selectivity could reach 53%, much higher than that of 23% over fresh SAPO-34 catalyst. Several characterizations, e.g., Fourier transform infrared spectroscopy and gas chromatography–mass spectrometry, indicated that methylated benzenes, which were active hydrocarbon pool species and prompted ethylene selectivity, presented as the main species of residual coke in the SAPO-34 catalyst regenerated via steam gasification. Meanwhile, oxygenated compounds and naphthalene, which could accelerate catalyst deactivation, were observed in the SAPO-34 catalyst partially regenerated via air combustion. This finding improved our understanding of the role of residual coke in the MTO reaction and provided a potential regeneration method for the industrial MTO process.



## 1. INTRODUCTION

The methanol-to-olefins (MTO) reaction, which provides a nonpetrochemical route for producing the lower olefins, has been successfully industrialized in China.<sup>1</sup> In MTO reaction, the SAPO-34 catalyst is commonly used and exhibits excellent catalytic selectivity to lower olefins because of its small eight-membered-ring pore opening.<sup>2</sup> However, the MTO reaction over the SAPO-34 catalyst is accompanied by a quick coke deposition that covers the acid sites and readily blocks the zeolite channels, causing deactivation of the catalyst.<sup>1,3,4</sup> Consequently, regeneration is an indispensable step to restoring the activity of the deactivated SAPO-34 catalyst in the MTO process.

In the industrial MTO process, a fluidized-bed reactor–regenerator configuration has been designed; thus, circulation of the catalyst can be established. In this way, the spent catalyst from the reactor can be transported to the regenerator to restore the catalytic activity by coke combustion with air or oxygen at temperatures of around 620–700 °C.<sup>1,5</sup> The “hydrocarbon pool” (HCP) mechanism proposed by Dahl and Kolboe<sup>6</sup> illustrated that the active aromatic species could act as cocatalysts to accelerate methanol conversion but also exert a noticeable effect on the product distribution. Hence, a reasonable way to enhance lower olefin selectivity is to partly remove the coke and retain a certain amount of coke inside the zeolite pores. However, coke combustion is a rapid and yet

highly exothermic reaction,<sup>7</sup> and strict control of partial catalyst regeneration, that is, controlling an appropriate coke combustion rate, is a challenge.

Because the coke species trapped in the SAPO-34 catalyst during the MTO reaction are closely related to the HCP mechanism and have an effect on the reaction and deactivation, therefore control of the coke property is an interesting way of improving the MTO process. Some previous studies indicated that the gas used for coke removal has a significant influence on the regeneration rate and properties of residual coke.<sup>8–11</sup> It has been demonstrated that the regeneration rate of gas in coke removal of the deactivated alumina-supported cobalt–nickel catalyst and metallurgical coke followed the order of air  $\gg$  H<sub>2</sub>O(g) > CO<sub>2</sub>  $\gg$  H<sub>2</sub> > N<sub>2</sub>.<sup>12,13</sup> This clearly shows that the combustion rate of air is the fastest, while the regeneration rates of steam [H<sub>2</sub>O(g)], CO<sub>2</sub>, and H<sub>2</sub> are slower and thus more controllable. In fact, it has been anticipated that steam can act as the active agent in hydrogenation, thus avoiding dehydrogenation of the coke and causing catalyst rejuvenation.<sup>9,10</sup> Thus, steam can be used to remove coke deposited in the catalyst, which has been

Received: August 29, 2018

Revised: November 26, 2018

Accepted: December 3, 2018

Published: December 3, 2018

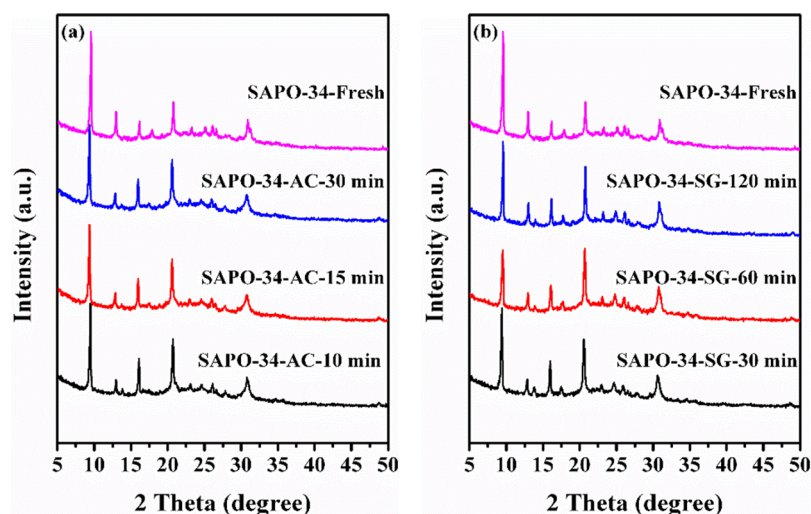


Figure 1. XRD patterns of the fresh, SAPO-34-AC (a) and SAPO-34-SG samples (b).

confirmed in the regeneration of a spent equilibrium catalyst in the fluid catalytic cracking process,<sup>14,15</sup> the conversion of cracking-formed coke in a bifunctional catalyst to syngas in the petroleum residue cracking gasification process,<sup>16</sup> and the gasification of carbon deposits on a nickel catalyst.<sup>17</sup>

In this work, we studied the partial regeneration of spent SAPO-34 catalysts by use of steam in the MTO process, especially the effect of such partial regeneration on the product distribution of the MTO reaction. First, the spent SAPO-34 catalyst was partially regenerated by steam gasification. Then, the impact of the content of the residual coke on the MTO performance was evaluated under the same operation conditions in a fluidized-bed reactor at atmospheric pressure. We also compared the catalytic performance of the MTO reaction over catalysts partially regenerated by steam gasification with that by air combustion to highlight the superiority of the method of steam gasification. Meanwhile, we also attempted to provide mechanistic insights into the performance, in particular the relatively high selectivity to ethylene over SAPO-34 catalysts partially regenerated by steam gasification. The partially regenerated SAPO-34 catalysts were characterized by thermogravimetric analysis, N<sub>2</sub> adsorption/desorption, Fourier transform infrared spectroscopy, temperature-programmed desorption of ammonia, and gas chromatography–mass spectrometry, which favored elucidation of the nature of the residual coke retained inside the SAPO-34 catalyst by different regeneration methods and their correlation with the catalytic performance in the MTO process. In this regard, a better understanding of the residual coke and its role in the MTO reaction mechanism and deactivation is expected.

## 2. EXPERIMENTAL SECTION

**2.1. Catalyst Preparation.** In this study, the catalyst used was the industrial MTO SAPO-34 catalyst.<sup>1</sup> To remove the template agent, all of the catalysts were calcined at 650 °C in air for 6 h before the experiment.

**2.2. Catalyst Characterization.** X-ray diffraction (XRD) measurements were conducted to characterize the crystallographic structures of the samples. The data were collected in the  $2\theta$  range of 0–50°.

The temperature-programmed desorption of ammonia (NH<sub>3</sub>-TPD) was carried on a Micromeritics Autochem II 2920 instrument to characterize the acid distribution on the

SAPO-34 catalyst. Samples were pretreated at 600 °C for 1 h and then cooled to 100 °C. After saturation with NH<sub>3</sub> gas, NH<sub>3</sub>-TPD was carried out from 100 to 600 °C.

The total and residual coke contents were measured with thermogravimetric analysis (TGA). The samples were heated in flowing air from room temperature to 900 °C at a heating rate of 10 °C/min with an air flow rate of 100 mL/min.

The N<sub>2</sub> adsorption/desorption measurements were carried out on a Micromeritics ASAP2020 setup. Prior to measurement, the samples were degassed at 350 °C under vacuum for 4 h. The total surface area and pore volume were calculated based on the Brunauer–Emmett–Teller (BET) equation and t-plot method.

The concentration of acid sites of different samples was quantified by Fourier transform infrared spectroscopy (FTIR) using NH<sub>3</sub> as the probe molecule. Spectra were recorded on a Tensor spectrometer with a resolution of 4 cm<sup>-1</sup>. The samples were pressed into self-supporting wafers and pretreated in vacuum at 450 °C for 1 h (in order to remove volatile species). All spectra were collected at 150 °C. NH<sub>3</sub> adsorption was carried out at 150 °C for 0.5 h, followed by 0.5 h of evacuation to remove physical adsorption of NH<sub>3</sub>.

The soluble coke species of residual coke were determined following the Guisnet method. Typically, 50 mg of sample was dissolved in 1.0 mL of 15% hydrogen fluoride in a screw-cap Teflon. The addition of 1 mL of CH<sub>2</sub>Cl<sub>2</sub> with C<sub>2</sub>Cl<sub>6</sub> as the internal standard allowed extraction of the soluble fraction of coke. The CH<sub>2</sub>Cl<sub>2</sub> solution was identified with an Agilent 7890 A/5975C gas chromatography–mass spectrometry (GC-MS) instrument.

**2.3. Experimental Setup.** The experiments of the MTO reaction and regeneration of spent catalysts were both carried out in a fluidized-bed reactor made of quartz, instead of steel, to avoid thermal decomposition of methanol on the metal well. The reactor had an inner diameter of 0.019 m and a height of 0.35 m. For each experiment, 5 g of catalyst was loaded into the reactor. The gas product was in situ analyzed with an Agilent 7890A gas chromatograph equipped with a flame ionization detector and a PorapLOT Q-HT capillary column (25 m × 0.53 mm × 0.02 mm).

**2.4. MTO Reaction and Partial Regeneration Experiments.** The MTO reaction experiments were carried out under 490 °C with a weight hourly space velocity (WHSV, i.e.,

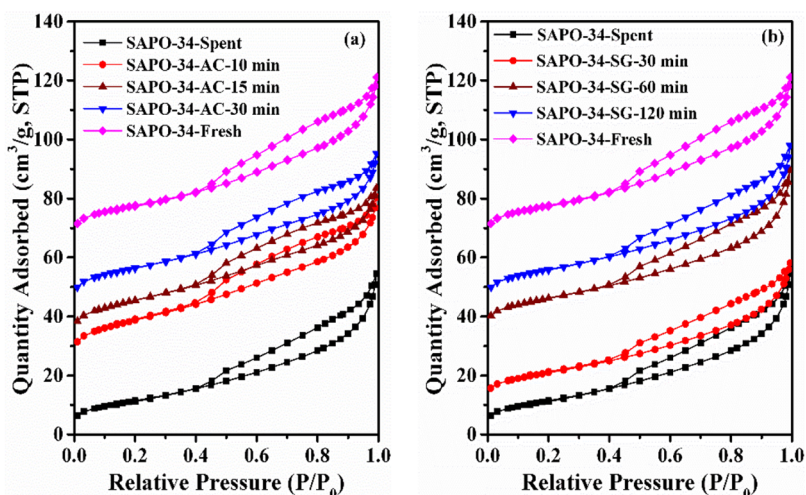


Figure 2.  $N_2$  adsorption/desorption isotherms of the fresh, spent, and SAPO-34-AC (a) and SAPO-34-SG (b) samples.

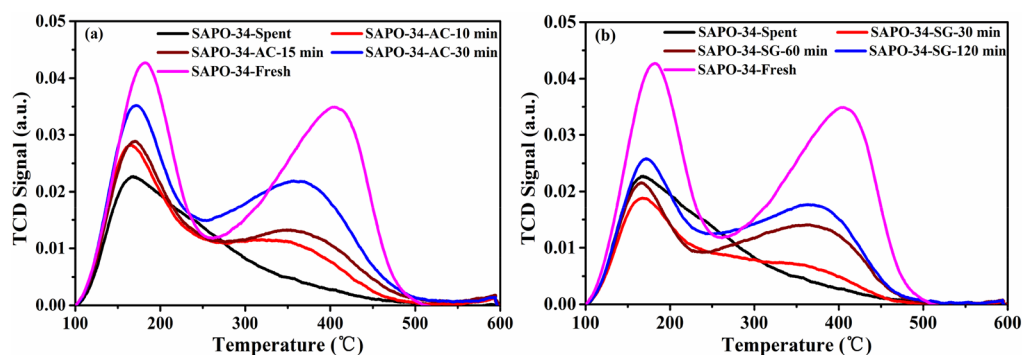


Figure 3.  $NH_3$ -TPD profiles of fresh, spent, and SAPO-34-AC (a) and SAPO-34-SG (b) samples.

the ratio of the feed rate of methanol to catalyst loading) of  $2 \text{ h}^{-1}$  and a ratio of water to methanol in the feed of 0.25. To achieve the same degree of coke deposition, each MTO reaction proceeded for 110 min over the fresh SAPO-34 catalyst, reaching a methanol conversion of less than 20%. After the MTO reaction, the spent catalyst was heated to a specific temperature and aged for 15 min and then kept for a different time on the same experimental apparatus to achieve partial regeneration with either air or steam. Then the regenerated catalyst was cooled to  $490 \text{ }^\circ\text{C}$  to study the effect of partial regeneration on the MTO reaction. In order to reduce the reaction rate in the regeneration by air combustion, air was diluted four times by  $N_2$ , ensuring constant total gas velocity.

In this work, SAPO-34-AC means spent SAPO-34 catalyst regenerated by air combustion at  $550 \text{ }^\circ\text{C}$  with a WHSV of  $3 \text{ h}^{-1}$ , and SAPO-34-SG represents spent SAPO-34 catalyst regenerated by steam gasification at  $680 \text{ }^\circ\text{C}$  with a WHSV of  $3 \text{ h}^{-1}$ . Fresh SAPO-34 and spent SAPO-34 catalysts without regeneration are denoted as SAPO-34-Fresh and SAPO-34-Spent, respectively.

### 3. RESULTS AND DISCUSSION

**3.1. Characterization of the Fresh and Partially Regenerated Catalysts.** The crystal structures of the spent SAPO-34 after air combustion and steam gasification for different times are examined by powder XRD patterns, as shown in Figure 1. After partial regeneration, all of the samples showed a relatively high crystallinity of 97–100% (Table S1)

and exhibited the characteristic peaks of a typical chabazite structure at  $2\theta$  values of  $9.40^\circ$ ,  $12.79^\circ$ ,  $15.90^\circ$ ,  $17.53^\circ$ ,  $20.45^\circ$ , and  $30.85^\circ$ ,<sup>18</sup> indicating that the partial regeneration by air combustion and steam gasification did not impair the integrity of the crystalline structure of SAPO-34. This was consistent with the excellent hydrothermal stability of the SAPO-34 catalyst.<sup>19,20</sup>

Figure 2 compares the physisorption isotherms of the fresh and partially regenerated samples as determined by  $N_2$  adsorption/desorption, and the corresponding textural properties (pore volume and specific surface area) are summarized in Table S2. After partial regeneration, the physical properties of the catalysts were restored to a certain extent compared with the fresh catalyst. As expected, the longer the regeneration time, the higher the recovery degree of the pore structure. This phenomenon was independent of the regeneration gas and only related to the regeneration time.

Acidity is a crucial parameter that affects the product distribution for the MTO reaction, and the acid properties of the SAPO-34 samples before and after partial regeneration are evaluated by the  $NH_3$ -TPD technique. As shown in Figure 3, the acid amount and strength of the partially regenerated samples were restored to some certain degree. For both the SAPO-34-AC and SAPO-34-SG samples, there were two peaks centered at around 100–250 and 250–500  $^\circ\text{C}$ . The peak at higher temperature generally corresponds to the adsorption of  $NH_3$  on the strong acid sites, and the peak at lower temperature corresponds to the physisorption of  $NH_3$  or the adsorption of  $NH_3$  on the weak acid sites.<sup>21,22</sup> Quantitative

evolution of the catalyst acidity is presented in Table S3. The longer the regeneration time, the more the total acid amount recovered, as shown in Figure 3 and Table S3. Compared to the SAPO-34-Fresh sample, the high-temperature peak of the partially regenerated samples shifted to lower temperature, indicating that the strength of the strong acid became weak.

Although steam is widely used in industrial operations and can be of use in the gasification of coke,<sup>23</sup> the hydrothermal stability of the catalyst should be taken into account when steam is selected as the regeneration gas because steam is prone to attacking the Al–O bond of the crystal under higher-temperature conditions and then steadily destroying the crystal structure of zeolite, such as HZSM-5,<sup>24</sup>  $\beta$ ,<sup>25</sup> HY,<sup>26</sup> and so on. Watanabe et al. found that SAPO-34 zeolites were hydrothermally stable up to 1000 °C even under almost pure steam conditions.<sup>19</sup> Liu et al. also found that the crystal structure of the SAPO-34 catalyst was well-reserved after treatment by 100% steam at 800 °C for 24 h.<sup>20</sup> Apparently, the excellent hydrothermal stability of SAPO-34 means that it is feasible to remove coke by steam gasification under the operation conditions in this work.

**3.2. Regeneration Rate of Air Combustion and Steam Gasification.** The residual coke content after partial regeneration is one of the crucial parameters that determine the initial catalytic activity but depend on the regeneration rate. The coke content versus regeneration time is plotted in Figure 4. The coke content of the SAPO-34 catalyst after the

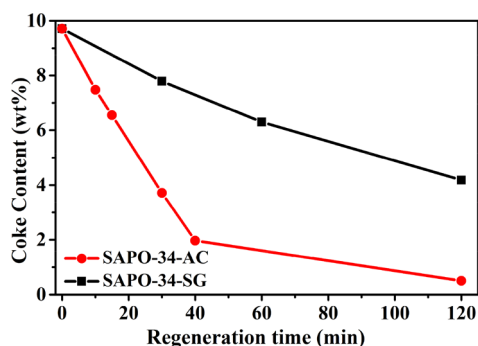


Figure 4. Variations of the residual coke content with the regeneration time for the SAPO-34-AC and SAPO-34-SG samples.

MTO reaction was measured by TGA to be 9.7 wt %. When the spent catalyst was regenerated by air combustion, the coke content quickly decreased to 3.7% within 30 min at 550 °C with a WHSV of 3 h<sup>-1</sup>. Moreover, the regeneration rate increased with increasing regeneration temperature.<sup>5</sup> Therefore, if partial regeneration with air combustion is used for

industrial practice, careful control of the regeneration rate has to be considered. The rate of coke removal, however, is much slower with steam gasification as the regeneration method. In this case, the coke content on the regenerated SAPO-34 catalyst was still 6.3% after 60 min and 4.2% after 120 min. Although air combustion was quite effective at removing the coke, it was hard to control the reaction rate, thus controlling the residual coke content, which would, in turn, influence the MTO performance. The moderate regeneration rate of steam gasification, however, made it possible to obtain a desired residual coke content in the regenerated SAPO-34 catalyst via a partial regeneration strategy.

**3.3. Catalytic Performance of the Partially Regenerated Catalysts.** Although the pore structure and acid amount have been restored to some extent for partially regenerated catalysts, it is not yet known how the partially regenerated catalyst behaves during the MTO reaction. Therefore, the first open question now is whether partial regeneration can restore the catalytic activity and even alter the product selectivity. In the following study, these partially regenerated samples will be tested to explore the effect of residue coke on the MTO performance. The efficiency of partial regeneration will be assessed.

**3.3.1. Effect of the Residual Coke Content on the Product Distribution of the MTO Reaction.** According to the previous studies, the coke content can strongly influence the product distribution of the MTO reaction.<sup>1,27,28</sup> Therefore, to verify the effectiveness of the partial regeneration method, catalytic tests of the MTO reaction were performed over these partially regenerated catalysts with different residual coke contents. Table 1 provides the detailed initial product distribution on these samples. This was in stark contrast to the result obtained over the SAPO-34-Fresh sample, which displayed low activity. All partially regenerated SAPO-34 catalysts exhibited almost 100% methanol conversion but largely different product distributions, especially for ethylene. For the SAPO-34-AC samples, when the residual coke content increased from 3.71% to 7.48%, the ethylene selectivity increased from 36.4% to 49.3%. Similarly, for the SAPO-34-SG samples, when the residual coke content increased from 4.18% to 7.79%, the ethylene selectivity increased from 42.6% to 67.3%. These results were well consistent with the general observation that a certain amount of coke deposition could favor ethylene formation, which was traditionally ascribed to the result of product shape selectivity<sup>29,30</sup> or of transition-state shape selectivity<sup>31,32</sup> or due to the abundance of methylnaphthalene.<sup>33</sup> However, in a parallel work, we are trying to clarify this mechanism argument by combining GC–MS analysis and isotopic experiment with theoretical calculations. Our prelimi-

Table 1. Product Distribution of the MTO Reaction after a Time on Stream of 3 min for Both the SAPO-34-AC and SAPO-34-SG Samples Regenerated for Different Times

sample	conversion (%)	initial product distribution (%)							
		C <sub>1</sub> <sup>0</sup>	C <sub>2</sub> <sup>0</sup>	C <sub>3</sub> <sup>0</sup>	C <sub>2</sub> <sup>=</sup>	C <sub>3</sub> <sup>=</sup>	C <sub>4</sub> <sup>=</sup>	C <sub>5</sub> <sup>+</sup>	C <sub>2</sub> <sup>=</sup> + C <sub>3</sub> <sup>=</sup>
SAPO-34-Fresh	99.8	1.6	0.5	7.5	22.9	37.1	17.8	12.6	60.0
SAPO-34-AC-10 min	98.5	6.4	1.4	2.1	49.3	32.1	6.1	1.9	81.4
SAPO-34-AC-15 min	99.5	4.0	1.4	3.6	44.5	32.0	10.3	4.1	76.5
SAPO-34-AC-30 min	99.5	2.1	0.9	4.8	36.4	34.9	12.9	8.0	71.3
SAPO-34-SG-30 min	98.1	8.2	3.0	3.6	67.3	16.4	1.2	0.3	83.7
SAPO-34-SG-60 min	99.9	4.5	1.1	1.9	53.4	27.4	8.2	3.6	80.8
SAPO-34-SG-120 min	99.9	6.1	1.0	3.0	42.6	28.8	11.2	6.7	71.4

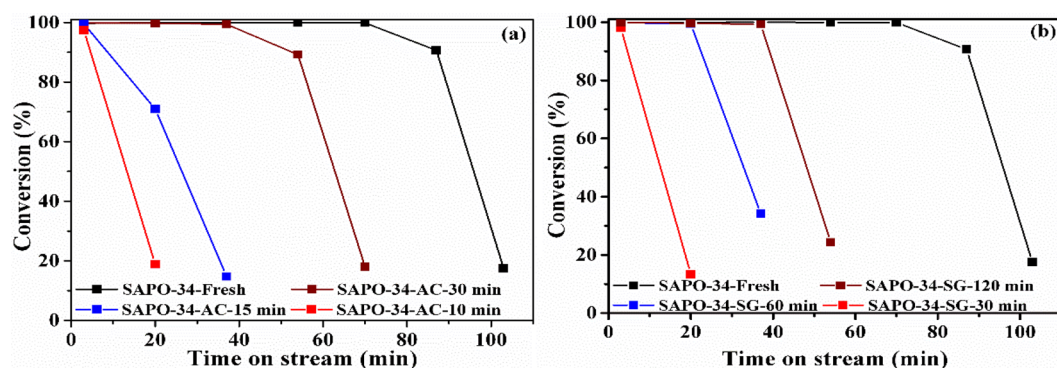


Figure 5. Methanol conversion against time on stream over the fresh, SAPO-34-AC (a) and SAPO-34-SG (b) samples.

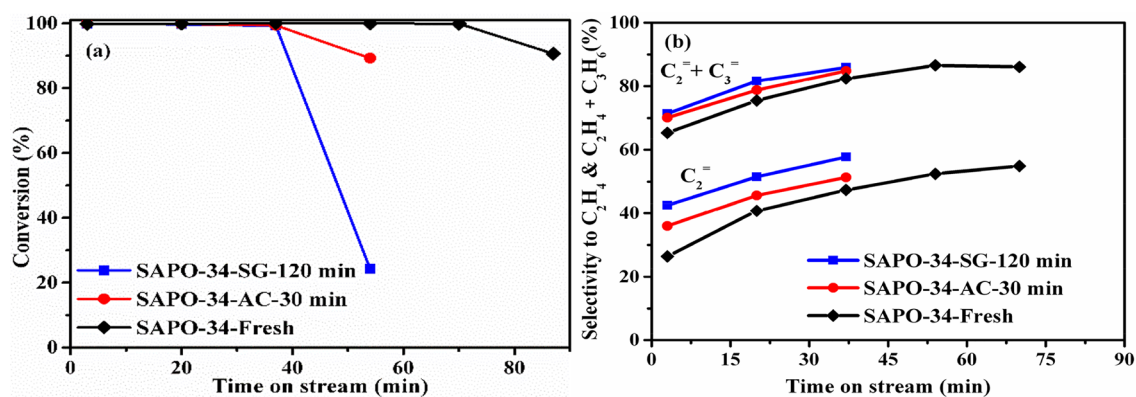


Figure 6. Methanol conversion (a) and product selectivity (b) versus time on stream during the MTO reaction over fresh and partially regenerated SAPO-34 catalysts.

nary results showed that the ethylene increase with coke deposition originates from the extension of the reaction zone inward of the crystal, which renders the diffusion-hindered higher olefins evolving to active aromatic species, thus prompting the aromatics–ethylene route. Besides, it was interesting to find that not only did ethylene show relatively higher selectivity with increasing residual coke content but so did methane, which was attributed to the reaction between the surface methoxy group and coke molecules.<sup>34</sup>

In contrast, compared with the SAPO-34-Fresh sample, SAPO-34-AC and SAPO-34-SG samples showed a remarkable decrease in selectivity to longer-chain ( $C_4^+$ ) hydrocarbons. The residual coke led to the modification of texture (Table S2), which might hinder the diffusion of longer-chain ( $C_4^+$ ) molecules. However, the propylene selectivity was relatively independent of the residual coke content, except for the SAPO-34-SG-30 min sample.

As discussed above, the residue coke has a significant positive impact on the initial product distribution, and enhanced initial ethylene selectivity was successfully realized with increasing residual coke content. However, besides the initial catalytic selectivity, attention should be paid to the catalyst lifetime.

The methanol conversion versus time on stream is shown in Figure 5. For the SAPO-34-Fresh sample, the catalyst lifetime with a 100% conversion of methanol could be maintained up to 70 min. However, the methanol conversions of those partially regenerated samples started to decrease much earlier. As shown in Figure 5a,b, the catalyst lifetime substantially increased with increasing regeneration time. For both the SAPO-34-AC-10 min and SAPO-34-SG-30 min samples, the

initial lower olefin selectivity (ethylene and propylene) could be increased up to 81%, but it was achieved at the expense of the catalyst lifetime, where the initial methanol conversion was lower than 98% and both samples deactivated rapidly. Fortunately, when the appropriate regeneration time (corresponding to the appropriate amount of residual coke) was chosen, a relatively longer catalyst lifetime can be achieved while a higher ethylene selectivity can also be maintained. The SAPO-34-AC-30 min and SAPO-34-SG-120 min samples had a stable methanol conversion of 99% for more than 38 min, while the formation of ethylene was still favored (Table 1 and Figure 5).

The enhanced ethylene selectivity was related to not only the residual coke content but also the regeneration gas. To get detailed information on the effect of the residual coke with different regeneration gases on the MTO reaction and catalyst deactivation, in the next section, we will compare the catalytic performances of the MTO reaction over the SAPO-34-AC and SAPO-34-SG samples with the nearly same residual coke content.

**3.3.2. Effect of the Regeneration Gas on the Product Distribution of the MTO Reaction.** Figure 6 shows the catalytic performances of the SAPO-34-AC-30 min and SAPO-34-SG-120 min samples (the corresponding residual coke contents were 3.71% and 4.18%, respectively) compared with the SAPO-34-Fresh sample for the MTO process. As shown in Figure 6a, the SAPO-34-AC-30 min sample had a slightly longer catalyst lifetime compared with the SAPO-34-SG-120 min sample, while for both catalysts, the catalyst lifetime with methanol conversion of >99% could be maintained up to 40 min. Figure 6b shows that a remarkable increase in the

ethylene selectivity, especially the initial ethylene selectivity, is realized over both partially regenerated samples. The initial selectivity to ethylene was 23% over the SAPO-34-Fresh sample. For the SAPO-34-AC-30 min sample, the selectivity of ethylene was enhanced to 36%. In particular, the selectivity to ethylene could reach as high as 43% for the SAPO-34-SG-120 min sample, 2-fold higher than the fresh catalyst. Meanwhile, the ethylene selectivity increased from 43% at 3 min to 58% at 38 min before the loss of catalytic activity. Moreover, the lower selectivity for SAPO-34-SG-120 min samples for 3 min was similar to that for the SAPO-34-Fresh sample for 20 min and the SAPO-34-AC-30 min sample for 3 min, but the  $C_2^=/C_3^=$  ratio was 1.48, 1.11, and 1.06, respectively, indicating that the SAPO-34-SG-120 min sample was more favorable for ethylene formation.

When the residual coke content of the SAPO-34-SG sample is elevated, the catalyst lifetime has been attenuated, as shown in Figure 5. The catalytic performances during the MTO reaction over the SAPO-34-SG-60 min and SAPO-34-SG-120 min samples with different residual coke contents are compared in Figure 7. When the regeneration time was

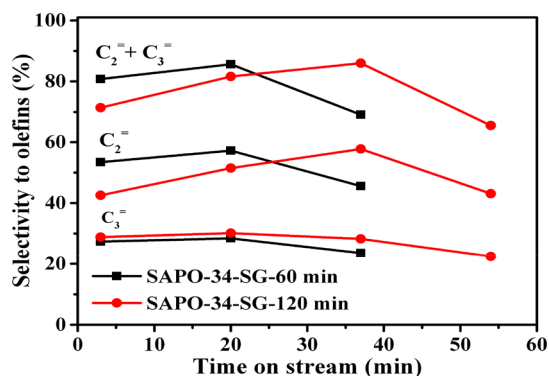


**Figure 7.** Product selectivity versus time on stream during the MTO reaction over the SAPO-34-SG-60 min and SAPO-34-SG-120 min samples. The corresponding methanol conversion can be found in Figure 5b.

shortened to 60 min, the optimal performance of the MTO reaction was achieved, which yielded a high initial lower olefin to 81%, and the highest selectivity of lower olefins of 87% was attained in a shorter reaction time (20 min) than the SAPO-34-SG-120 min sample for 38 min. Special attention should be paid to the ethylene selectivity, because propylene selectivity was essentially constant during the MTO reaction, approximately 29%. In contrast, the ethylene selectivity increased from 53% at 3 min to 58% at 20 min. In a nutshell, as long as the SAPO-34 catalyst has been regenerated for a suitable time, an optimal operation window for the industrial unit would be identified, in which a weak dependence on the age distribution of the catalyst as well as a high ethylene selectivity could be obtained.

**3.4. Mechanistic Understanding of the MTO Reaction Performance over the SAPO-34 Catalyst Partially Regenerated via Different Methods.** In order to understand the underlying mechanisms, we studied the pore structures, acidity properties, and coke compositions for the fresh SAPO-34 catalyst and spent catalysts partially regenerated via steam gasification or air combustion. Moreover, the regeneration rate and diffusion were also discussed.

**3.4.1. Assessing Textural and Acidic Properties for Different Partially Regenerated Samples.** In Table S2, we first compared the surface areas, micropore volumes, and mesopore volumes for different samples. A careful check of these three parameters showed that, compared to the fresh SAPO-34 sample, the mesopore volumes for both the SAPO-34-AC-30 min and SAPO-34-SG-120 min samples were almost recovered, indicating that the residual coke was largely occupied in the micropore channels. Meanwhile, it was found that the surface area, micropore volume, and mesopore volume of the SAPO-34-AC-30 min sample were  $S_{\text{BET}} = 190.3 \text{ m}^2/\text{g}$ ,  $V_{\text{micro}} = 0.065 \text{ cm}^3/\text{g}$ , and  $V_{\text{meso}} = 0.070 \text{ cm}^3/\text{g}$ , respectively, which agreed well with the corresponding results for the SAPO-34-SG-120 min sample, i.e.,  $S_{\text{BET}} = 188.4 \text{ m}^2/\text{g}$ ,  $V_{\text{micro}} = 0.065 \text{ cm}^3/\text{g}$ , and  $V_{\text{meso}} = 0.071 \text{ cm}^3/\text{g}$ . In addition, both the SAPO-34-AC-30 min and SAPO-34-SG-120 min samples manifested very similar adsorption/desorption isotherms, as shown in Figure S1, which meant that the physical structures of two spent catalysts partially regenerated via steam gasification and air combustion, respectively, exhibited a good enough similarity. This may suggest that the mechanism of ethylene promotion in the MTO reaction over the spent catalyst partially regenerated via steam gasification is not subject to changes of the physical structure of the catalyst.

To determine the nature of the active sites and their total acidity, both  $\text{NH}_3$ -TPD and the FTIR spectra were used in this work. The  $\text{NH}_3$ -TPD profiles of both partially regenerated samples are shown in Figure S2a. The results of  $\text{NH}_3$ -TPD show that the SAPO-34-SG-120 min sample exhibits lower acidic concentration in strong acidic sites compared with the SAPO-34-AC-30 min sample. Figure S2b shows the results of the FTIR spectra of adsorbed  $\text{NH}_3$ . As indicated by Jong et al.,<sup>35</sup> the integrated area of the band at  $3600 \text{ cm}^{-1}$  could be used to quantify the concentration of Brønsted acid. The intensity of the SAPO-34-AC-30 min sample was obviously higher than that of the SAPO-34-SG-120 min sample, suggesting a lower recovery of the acid of the SAPO-34-SG-120 min sample. These results reflected that the SAPO-34-SG-120 min sample possessed lower acidity than the SAPO-34-AC-30 min sample even though both samples had almost the same coke contents and pore structures. This discrepancy might be related to the fact that coke removal by air combustion was a selective process, in which the coke formed near the Brønsted acid sites were preferentially removed.<sup>35</sup>

It is anticipated that a lower acid density favors selectivity to propylene and higher olefins, which are formed mainly by the alkene-based reaction route.<sup>3,36</sup> However, in this work, the SAPO-34-SG-120 min sample with lower acid density could also lead to higher selectivity to ethylene. Therefore, enhanced selectivity to ethylene in the MTO reaction over the spent catalyst partially regenerated via steam gasification might not be attributed to the change of the catalyst acidity. Moreover, both partially regenerated samples exhibit similar textural properties, and thus the difference of the catalytic performances in the MTO reaction between these two partially regenerated SAPO-34 catalysts should be irrelevant to their textural properties. As discussed above, the difference between the acidities of both samples also cannot convincingly explain the differences in the product distribution. Therefore, enhanced selectivity to ethylene in the MTO reaction over the spent catalyst partially regenerated via steam gasification could not be related to the change of the pore structures and acidity properties.

**3.4.2. Characterization of the Nature of the Residual Coke for Different Partially Regenerated Catalysts.** It is well recognized that the nature of coke is of importance for the catalytic performance in the MTO reaction. To study the nature of residual coke, TGA, FTIR, and GC–MS experiments were conducted for three SAPO-34 catalyst samples: SAPO-34-Spent, SAPO-34-AC-30 min, and SAPO-34-SG-120 min.

We first attempted to derive the H/C of the residual coke in the spent SAPO-34 catalyst. It is hard to directly measure the H/C of residual coke in the spent SAPO-34 catalyst. Fortunately, it is possible to use both TGA and GC–MS to qualitatively study the change in H/C of residual coke. In TGA measurement, basically hydrogen-poor coke components, i.e., with lower H/C, are burned at a higher temperature ( $T_{G,max}$ ).<sup>37,38</sup> Figure 8 shows the differential thermogravimetry

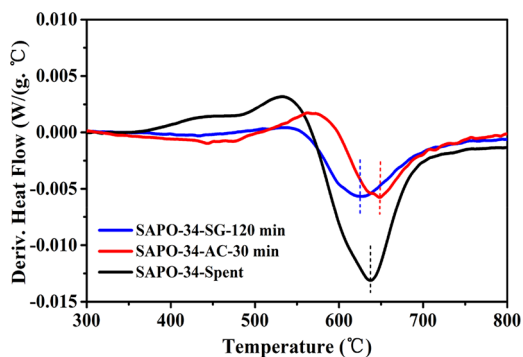


**Figure 8.** DTG profiles of partially regenerated SAPO-34 samples and the spent SAPO-34 sample.

(DTG) profiles for three samples. As can be seen,  $T_{G,max}$  for the SAPO-34-Spent, SAPO-34-AC-30 min, and SAPO-34-SG-120 min samples were 637, 643, and 625 °C, respectively. This suggested that the H/C of residual coke would decrease when the spent SAPO-34 catalyst was partially regenerated by air combustion and increase when partially regenerated by steam gasification.

As is well-known, the retained coke species can be analyzed by GC–MS and classified as soluble and insoluble coke. Table 2 shows the percentage of soluble and insoluble coke. In

**Table 2. Soluble and Insoluble Coke Contents and Their Ratio of Partially Regenerated Samples and the Spent SAPO-34 Sample**

sample	soluble coke (wt %)	insoluble coke (wt %)	soluble/insoluble ratio
SAPO-34-Spent	3.56	6.15	0.58
SAPO-34-AC-30 min	0.31	3.39	0.09
SAPO-34-SG-120 min	1.65	2.53	0.66

principle, the soluble coke is rich in lower polyaromatic species (i.e., higher H/C), whereas the insoluble coke is mainly heavier polyaromatic or graphitic species (i.e., lower H/C). Thus, the ratio of soluble and insoluble coke can represent qualitatively the change of H/C in coke. When the spent SAPO-34 catalyst was partially regenerated via air combustion, the ratio of soluble and insoluble coke changed from 0.58 for the SAPO-34-Spent sample to 0.09 for the SAPO-34-AC-30 min sample, which indicated the species in coke shifted toward insoluble

coke, i.e., lower H/C. When the spent SAPO-34 catalyst was partially regenerated via steam gasification, the ratio increased from 0.58 to 0.66, which suggested that the species in coke were hydrogen-rich and H/C increased. The results are in good agreement with the TGA measurements and confirm that the residual coke after partial regeneration by steam gasification has a nature different from that regenerated by air combustion.

To further discover the nature of the residual coke, we analyzed the main vibration bands corresponding to the carbon deposit region (Figure 9a) by FTIR. In principle, the absorptions at 1360–1470  $\text{cm}^{-1}$  can be attributed to alkyl branches of the aromatics, and the bands at 1500–1650  $\text{cm}^{-1}$  can be related to the stretching of aromatic rings.<sup>39</sup> It was worth noting that the appearance of bands at 1725–1745  $\text{cm}^{-1}$  for the SAPO-34-AC-30 min sample represents the  $\nu(\text{C}=\text{O})$  vibration of carboxylic acids.<sup>40</sup> Thus, it could be concluded that the residual coke in the SAPO-34-AC-30 min sample contained aromatics and oxygenated compounds. However, for the SAPO-34-SG-120 min sample, the bands at 1725–1745  $\text{cm}^{-1}$  were not detected, indicating that the residual coke contains only aromatics. To further elucidate the components of the residual coke, the soluble chemical compositions of the organic compounds retained in different samples were analyzed by GC–MS, and the results are shown in Figure 9b. As can be seen, large unsaturated aromatic hydrocarbons (phenanthrene, pyrene, and their derivatives) formed by hydride transfer and methylation<sup>41</sup> were mainly observed in the SAPO-34-Spent sample. For the SAPO-34-SG-120 min sample, a broad distribution of species, ranging from methylated benzenes to methylated naphthalenes and excluding the oxygenated compounds, were observed. Meanwhile, the oxygenated compounds and naphthalene were found to be dominant for the SAPO-34-AC-30 min sample. The results obtained by GC–MS were consistent with FTIR analysis, as shown in Figure 9a. Similarity, various oxygenated species, such as ketonic, aldehydic, and phenolic compounds, have been identified in partially oxidized samples of coked HY and HZSMS zeolites.<sup>8,42</sup> Therefore, the nature of the residual coke in the spent catalyst will be changed if different regeneration methods are applied.

**3.4.3. Role of the Residual Coke in the MTO Reaction.** It can be hypothesized from the above results that the performance of the ethylene selectivity in the MTO reaction over the spent catalyst partially regenerated via different methods might be due to the formation of different species in the residual coke during regeneration. In the residual coke of the SAPO-34-AC-30 min sample, the oxygenated compounds and naphthalene are dominant components. The role of oxygenated compounds in the MTO or MTH reaction has been previously investigated.<sup>43–45</sup> Liu et al.<sup>44</sup> found that oxygenated compounds could accelerate catalyst deactivation and only had a minor impact on the aromatic cycle that was decisive to the selectivity to ethylene in the MTO reaction. Müller et al.<sup>45</sup> confirmed that oxygenated compounds could be strongly adsorbed at Brønsted acid sites, then transformed to aromatic compounds, and caused rapid deactivation of the catalyst. In the meantime, for the SAPO-34-SG-120 min sample, the residual coke contains species ranging from methylated benzenes to methylated naphthalenes. It was found that methylated benzenes with fewer methyl groups had been considered as the active species, prompting ethylene

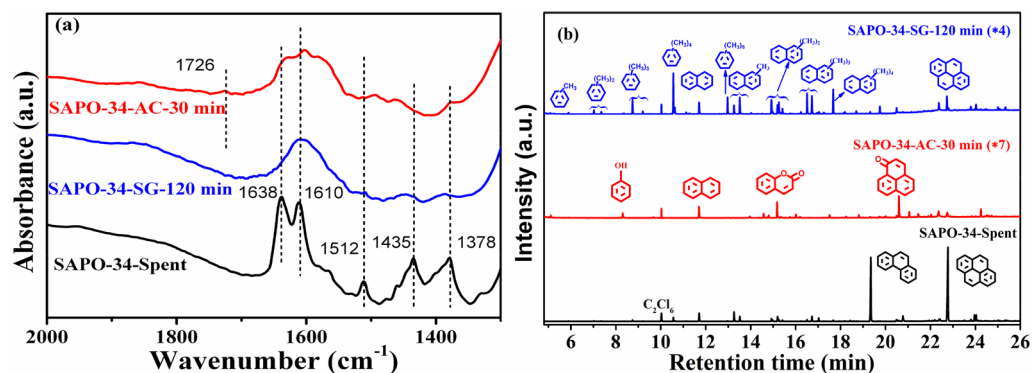


Figure 9. Residual coke characterization of SAPO-34 samples: (a) FTIR spectra; (b) GC-MS results.

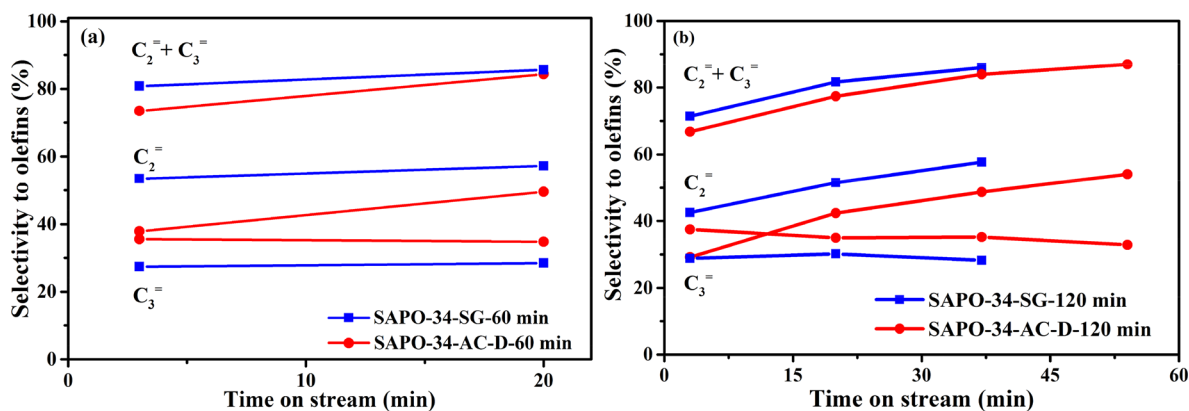


Figure 10. Catalytic performance of the MTO reaction over SAPO-34-SG and diluted air combustion (SAPO-34-AC-D) samples.

formation over HZSM-5<sup>46</sup> and SAPO-34<sup>32</sup> catalysts via the aromatic-based cycle.

It should be stressed that naphthalene and methylnaphthalene were found in the residual coke in both the SAPO-34-AC-30 min and SAPO-34-SG-120 min samples. It was reported that methylnaphthalene could also favor the formation of ethylene.<sup>33,32,47</sup> However, the activity of methylnaphthalene is only one-third that of methylbenzene, which makes methylnaphthalene the temporary intermediate in the MTO reaction and capable of being quickly masked by other more active compositions.<sup>33</sup> Borodina et al. found that methylnaphthalene was actually prone to forming deactivating species to shorten the catalyst lifetime in the MTO reaction at temperatures of 623–723 K.<sup>18</sup>

On the basis of the aforementioned discussions, we argue that the formation of methylated benzenes with fewer methyl groups in the residual coke of the spent SAPO-34 catalyst via steam gasification that has lower H/C can prompt ethylene selectivity.

**3.4.4. Effect of the Regeneration Rate and Diffusion on the MTO Performance.** Although we agree that the nature of the residual coke presents the main reason responsible for different performances in ethylene selectivity in the MTO reaction over spent catalysts partially regenerated via different methods, the influence of the regeneration rate and diffusion of guest molecules cannot be excluded.

From the results in Figure 4, we found that the reaction rate during regeneration by air combustion was nearly 4 times that by steam gasification. So, to ensure the same rate of coke removal, the air was diluted 4 times using N<sub>2</sub>, and the SAPO-34 catalyst partially regenerated by the diluted air was

abbreviated as SAPO-34-AC-D. The TGA results are shown in Figure S3. As can be seen, the residual coke content in SAPO-34-AC-D samples was slightly lower than that in SAPO-34-SG samples with the same regeneration time, which indicated that the coke removal rate by combustion of diluted air was nearly the same as that by steam gasification. The product distributions of the MTO reaction over spent catalysts partially regenerated by different methods are shown in Figure 10. The ethylene selectivity for SAPO-34-SG samples was higher than that with SAPO-34-AC-D samples, which was consistent with the results shown in Figure 6. The GC-MS results of SAPO-34-AC-D samples are shown in Figure S4, which also showed that the oxygenated compounds and naphthalene were still the main species of the residual coke for SAPO-34-AC-D samples. This indicates that the higher ethylene selectivity in the MTO reaction over the spent SAPO-34 catalyst partially regenerated by steam gasification is a consequence of the formation of active HCP species such as methylated benzenes, which is not due to the regeneration rate.

The BET results shown in Table S2 demonstrated that the coke was mostly located in the micropore channels. The higher the coke content, the smaller the free micropore volume, as shown in Table S2. This means that a serious pore blockage might exist, and the effective diffusivity of the guest molecules decreased as the coke content increased.<sup>48–50</sup> Li et al. found that the coke content had a significant influence on the self-diffusion coefficient of guest molecules: the self-diffusion coefficient of methane in ZSM-5 zeolite decreased almost linearly with an increase of the coke content.<sup>51</sup> Gao et al.<sup>50</sup> developed a reaction–diffusion model based on a dual-cycle reaction mechanism and Maxwell–Stefan diffusion theory for



the MTO reaction over the SAPO-34 catalyst. It was found that, for smaller molecules (methane), the apparent diffusion coefficient just slightly went down with increasing coke content, and for larger molecules such as  $C_4^+$ , the apparent diffusion coefficient decreased significantly at higher coke content. Our results in Table 1 confirmed that the selectivity to  $C_4^+$  decreased rapidly with increasing coke content. It is difficult to measure the diffusion coefficients of HCP species and oxygenated compounds in the SAPO-34 catalyst, which possesses a big challenge to directly connect the selectivity to ethylene with apparent diffusivities. However, as learned from Gao et al.,<sup>50</sup> the apparent diffusion coefficients for larger molecules, such as HCP species, would decrease significantly with increasing coke content, which might also enhance the diffusivity of ethylene and prompt the ethylene selectivity. This hypothesis, however, requires further experimental evidence.

In summary, the spent SAPO-34 catalyst partially regenerated by steam gasification was advantageous for the ethylene selectivity. On the basis of characterization analysis, the transformation of HCP species, i.e., oxygenated compounds, naphthalene, methylated benzene, and methylated naphthalene, was observed during partial regeneration by air combustion or steam gasification. However, steam was more effective than air because it could lead to the formation of more active HCP species such as methylated benzene, while air combustion mainly caused the formation of less active oxygenated compounds. Moreover, compared to air combustion, steam gasification of the coke can mitigate  $CO_2$  emission and simultaneously produce  $H_2$  and  $CO$ , which can be recycled as feedstocks for syngas in coal to an olefins plant.<sup>52</sup>

#### 4. CONCLUSION

In this work, we studied the partial regeneration of the spent SAPO-34 catalyst via both steam gasification and air combustion in the MTO process. The relationship between the residual coke content and catalytic performance in the MTO reaction was explored. It is shown that steam gasification is a more effective process than traditional air combustion in terms of prompting ethylene selectivity in the MTO reaction. By use of characterization methods such as  $NH_3$ -TPD,  $N_2$  adsorption/desorption, TGA, FTIR and GC-MS, we attempted to discover the underlying mechanism. It is found that methylated benzenes, which are active HCP species and prompt the ethylene selectivity, form as the main species of residual coke in the SAPO-34 catalyst regenerated via steam gasification. Regeneration via air combustion, however, mainly causes the formation of less active oxygenated compounds. In words, partial regeneration via steam gasification offers an efficient and economical method in enhancing the catalytic performance and utilizing the low-value coke.

#### ■ ASSOCIATED CONTENT

##### Supporting Information

The Supporting Information is available free of charge on the ACS Publications website at DOI: 10.1021/acs.iecr.8b04181.

Relative crystallinity, texture properties, acid properties, and compositions of coke of fresh, spent, and partially regenerated samples (PDF)

#### ■ AUTHOR INFORMATION

##### Corresponding Author

\*E-mail: maoye@dicp.ac.cn.

#### ORCID

Mao Ye: 0000-0002-7078-2402

Zhongmin Liu: 0000-0001-8439-2336

#### Notes

The authors declare no competing financial interest.

#### ■ ACKNOWLEDGMENTS

We are grateful to the National Natural Science Foundation of China (Grants 91334205 and 21703239).

#### ■ REFERENCES

- (1) Tian, P.; Wei, Y. X.; Ye, M.; Liu, Z. M. Methanol to olefins (MTO): from fundamentals to commercialization. *ACS Catal.* **2015**, *5*, 1922–1938.
- (2) Goetze, J.; Meirer, F.; Yarulina, I.; Gascon, J.; Kapteijn, F.; Ruiz-Martínez, J.; Weckhuysen, B. M. Insights into the activity and deactivation of the methanol-to-olefins process over different small-pore zeolites as studied with operando UV-vis spectroscopy. *ACS Catal.* **2017**, *7*, 4033–4046.
- (3) Chen, D.; Moljord, K.; Holmen, A. A methanol to olefins review: diffusion, coke formation and deactivation on SAPO type catalysts. *Microporous Mesoporous Mater.* **2012**, *164*, 239–250.
- (4) Haw, F.; Song, W. G.; Marcus, M.; Nicholas, B. The mechanism of methanol to hydrocarbon catalysis. *Acc. Chem. Res.* **2003**, *36*, 317–326.
- (5) Aguayo, A. T.; Gayubo, A. G.; Atutxa, A.; Olazar, M.; Bilbao, J. Regeneration of a catalyst based on a SAPO-34 used in the transformation of methanol into olefins. *J. Chem. Technol. Biotechnol.* **1999**, *74*, 1082–1088.
- (6) Dahl, I. M.; Kolboe, S. On the reaction mechanism for propylene formation in the MTO reaction over SAPO-34. *Catal. Lett.* **1993**, *20*, 329–336.
- (7) Keskitalo, T. J.; Lipiäinen, K. J. T.; Krause, A. O. I. Kinetic modeling of coke oxidation of a ferrierite catalyst. *Ind. Eng. Chem. Res.* **2006**, *45*, 6458–6467.
- (8) Moljord, K.; Magnoux, P.; Guisnet, M. Pyrene oxidation as a model reaction for characterizing the mechanism of coke oxidation on Y zeolites. *Catal. Lett.* **1994**, *28*, 53–59.
- (9) Aguayo, A. T.; Gayubo, A. G.; Ereña, J.; Atutxa, A.; Bilbao, J. Coke aging and its incidence on catalyst regeneration. *Ind. Eng. Chem. Res.* **2003**, *42*, 3914–3921.
- (10) Coll, R.; Salvado, J.; Farriol, X.; Montane, D. Steam reforming model compounds of biomass gasification tars: conversion at different operating conditions and tendency towards coke formation. *Fuel Process. Technol.* **2001**, *74*, 19–31.
- (11) Magnoux, P.; Cerqueira, H. S.; Guisnet, M. Evolution of coke composition during ageing under nitrogen. *Appl. Catal., A* **2002**, *235*, 93–99.
- (12) Guo, W. T.; Xue, Q. G.; Liu, Y. L.; Guo, Z. C.; She, X. F.; Wang, J. S.; Zhao, Q. Q.; An, X. W. Kinetic analysis of gasification reaction of coke with  $CO_2$  or  $H_2O$ . *Int. J. Hydrogen Energy* **2015**, *40*, 13306–13313.
- (13) Alenazey, F.; Cooper, C. G.; Dave, C. B.; Elnashaie, S. S. E. H.; Susu, A. A.; Adesina, A. A. Coke removal from deactivated Co–Ni steam reforming catalyst using different gasifying agents: An analysis of the gas–solid reaction kinetics. *Catal. Commun.* **2009**, *10*, 406–411.
- (14) Corma, A.; Sauvanaud, L.; Dorskocil, E.; Yaluris, G. Coke steam reforming in FCC regenerator: A new mastery over high coking feeds. *J. Catal.* **2011**, *279*, 183–195.
- (15) Zhang, Y. M.; Yu, D. P.; Li, W. L.; Wang, Y.; Gao, S. Q.; Xu, G. W. Fundamentals of petroleum residue cracking gasification for coproduction of oil and syngas. *Ind. Eng. Chem. Res.* **2012**, *51*, 15032–15040.
- (16) Zhang, Y. M.; Yu, D. P.; Li, W. L.; Gao, S. Q.; Xu, G. W. Bifunctional catalyst for petroleum residue cracking gasification. *Fuel* **2014**, *117*, 1196–1203.

- (17) Figueiredo, J. L.; Trimm, D. L. Gasification of carbon deposits on nickel catalysts. *J. Catal.* **1975**, *40*, 154–159.
- (18) Borodina, E.; Sharbini Harun Kamaluddin, H.; Meirer, F.; Mokhtar, M.; Asiri, A. M.; Althabaiti, S. A.; Basahel, S. N.; Ruiz-Martinez, J.; Weckhuysen, B. M. Influence of the reaction temperature on the nature of the active and deactivating species during methanol-to-olefins conversion over H-SAPO-34. *ACS Catal.* **2017**, *7*, 5268–5281.
- (19) Watanabe, Y.; Koiwai, A.; Takeuchi, H.; Hyodo, S. A.; Noda, S. Multinuclear NMR studies on the thermal stability of SAPO-34. *J. Catal.* **1993**, *143*, 430–436.
- (20) Liu, G. Y.; Tian, P.; Li, J. Z.; Zhang, D. Z.; Zhou, F.; Liu, Z. M. Synthesis, characterization and catalytic properties of SAPO-34 synthesized using diethylamine as a template. *Microporous Mesoporous Mater.* **2008**, *111*, 143–149.
- (21) Zhu, Q. J.; Kondo, J. N.; Tatsumi, T.; Inagaki, S.; Ohnuma, R.; Kubota, Y.; Shimodaira, Y.; Kobayashi, H.; Domen, K. A comparative study of methanol to olefin over CHA and MTF zeolites. *J. Phys. Chem. C* **2007**, *111*, 5409–5415.
- (22) Li, Z. B.; Martinez-Triguero, J.; Yu, J. H.; Corma, A. Conversion of methanol to olefins: Stabilization of nanosized SAPO-34 by hydrothermal treatment. *J. Catal.* **2015**, *329*, 379–388.
- (23) Mahamulkar, S.; Yin, K.; Agrawal, P. K.; Davis, R. J.; Jones, C. W.; Malek, A.; Shibata, H. Formation and oxidation/gasification of carbonaceous deposits: a review. *Ind. Eng. Chem. Res.* **2016**, *55*, 9760–9818.
- (24) Campbell, S. M.; Bibby, D. M.; Coddington, J. M.; Howe, R. F.; Meinhold, R. H. Dealumination of HZSM-5 zeolites: I. calcination and hydrothermal treatment. *J. Catal.* **1996**, *161*, 338–349.
- (25) Müller, M.; Harvey, G.; Prins, R. Comparison of the dealumination of zeolites beta, mordenite, ZSM-5 and ferrierite by thermal treatment, leaching with oxalic acid and treatment with SiCl<sub>4</sub> by <sup>1</sup>H, <sup>29</sup>Si and <sup>27</sup>Al MAS NMR. *Microporous Mesoporous Mater.* **2000**, *34*, 135–147.
- (26) Triantafyllidis, C. S.; Vlessidis, A. G.; Evmiridis, N. P. Dealuminated H–Y zeolites: influence of the degree and the type of dealumination method on the structural and acidic characteristics of H–Y zeolites. *Ind. Eng. Chem. Res.* **2000**, *39*, 307–319.
- (27) Chen, D.; Rebo, H. P.; Moljord, K.; Holmen, A. Influence of coke deposition on selectivity in zeolite catalysis. *Ind. Eng. Chem. Res.* **1997**, *36*, 3473–3479.
- (28) Qi, G. Z.; Xie, Z. K.; Yang, W. M.; Zhong, S. Q.; Liu, H. X.; Zhang, C. F.; Chen, Q. L. Behaviors of coke deposition on SAPO-34 catalyst during methanol conversion to light olefins. *Fuel Process. Technol.* **2007**, *88*, 437–441.
- (29) Hereijgers, B. P. C.; Bleken, F.; Nilsen, M. H.; Svelle, S.; Lillerud, K. P.; Bjørgen, M.; Weckhuysen, B. M.; Olsbye, U. Product shape selectivity dominates the Methanol-to-Olefins (MTO) reaction over H-SAPO-34 catalysts. *J. Catal.* **2009**, *264*, 77–87.
- (30) Dahl, I. M.; Wendelbo, R.; Andersen, A.; Akporiaye, D.; Mostad, H.; Fuglerud, T. The effect of crystallite size on the activity and selectivity of the reaction of ethanol and 2-propanol over SAPO-34. *Microporous Mesoporous Mater.* **1999**, *29*, 159–171.
- (31) Chen, D.; Moljord, K.; Fuglerud, T.; Holmen, A. The effect of crystal size of SAPO-34 on the selectivity and deactivation of the MTO reaction. *Microporous Mesoporous Mater.* **1999**, *29*, 191–203.
- (32) Song, W. G.; Fu, H.; Haw, F. J. Supramolecular origins of product selectivity for methanol-to-olefin catalysis on HSAPO-34. *J. Am. Chem. Soc.* **2001**, *123*, 4749–4754.
- (33) Song, W. G.; Fu, H.; Haw, F. J. Selective synthesis of methylnaphthalenes in HSAPO-34 cages and their function as reaction centers in methanol-to-olefin catalysis. *J. Phys. Chem. B* **2001**, *105*, 12839–12843.
- (34) Rostami, R. B.; Ghavipour, M.; Di, Z.; Wang, Y.; Behbahani, R. M. Study of coke deposition phenomena on the SAPO-34 catalyst and its effects on light olefin selectivity during the methanol to olefin reaction. *RSC Adv.* **2015**, *5*, 81965–81980.
- (35) Jong, S. J.; Pradhan, A. R.; Wu, J. F.; Tsai, T. C.; Liu, S. B. On the regeneration of coked H-ZSM-5 catalysts. *J. Catal.* **1998**, *174*, 210–218.
- (36) Xu, S. T.; Zhi, Y. C.; Han, J. F.; Zhang, W. N.; Wu, X. Q.; Sun, T. T.; Wei, Y. X.; Liu, Z. M. Advances in catalysis for methanol-to-olefins conversion. *Adv. Catal.* **2017**, *61*, 37–122.
- (37) Maldonado-Hódar, F. J.; Ribeiro, M. F.; Silva, J. M.; Antunes, A. P.; Ribeiro, F. R. Aromatization of n-heptane on Pt/Alkali or Alkali-Earth exchanged Beta zeolite catalysts: catalyst deactivation and regeneration. *J. Catal.* **1998**, *178*, 1–13.
- (38) Magnoux, P.; Guisnet, M.; Mignard, S.; Cartraud, P. Coking, aging, and regeneration of zeolites: VIII. Nature of coke formed on hydrogen offretite during n-heptane cracking: Mode of formation. *J. Catal.* **1989**, *117*, 495–502.
- (39) Wei, Y. X.; Zhang, D. Z.; Liu, Z. M.; Su, B. L. Highly efficient catalytic conversion of chloromethane to light olefins over HSAPO-34 as studied by catalytic testing and in situ FTIR. *J. Catal.* **2006**, *238*, 46–57.
- (40) Mariey, L.; Lamotte, J.; Chevreau, T.; Lavalley, J. C. FT-IR study of coked HY zeolite regeneration using oxygen or ozone. *React. Kinet. Catal. Lett.* **1996**, *59*, 241–246.
- (41) Schulz, H. Coking of zeolites during methanol conversion: basic reactions of the MTO-, MTP- and MTG processes. *Catal. Today* **2010**, *154*, 183–194.
- (42) Magnoux, P.; Guisnet, M. Coking, ageing and regeneration of zeolites: VI. comparison of the rates of coke oxidation of HY, H-Mordenite and HZSM-5. *Appl. Catal.* **1988**, *38*, 341–352.
- (43) Vogt, C.; Weckhuysen, B. M.; Ruiz-Martinez, J. Effect of feedstock and catalyst impurities on the methanol-to-olefin reaction over H-SAPO-34. *ChemCatChem* **2017**, *9*, 183–194.
- (44) Liu, Z. H.; Dong, X. L.; Liu, X.; Han, Y. Oxygen-containing coke species in zeolite-catalyzed conversion of methanol to hydrocarbons. *Catal. Sci. Technol.* **2016**, *6*, 8157–8165.
- (45) Müller, S.; Liu, Y.; Vishnuvarthan, M.; Sun, X. Y.; van Veen, A. C.; Haller, G. L.; Sanchez-Sanchez, M.; Lercher, J. A. Coke formation and deactivation pathways on H-ZSM-5 in the conversion of methanol to olefins. *J. Catal.* **2015**, *325*, 48–59.
- (46) Wang, C.; Xu, J.; Qi, G. D.; Gong, Y. J.; Wang, W. Y.; Gao, P.; Wang, Q.; Feng, N. D.; Liu, X. L.; Deng, F. Methylbenzene hydrocarbon pool in methanol-to-olefins conversion over zeolite H-ZSM-5. *J. Catal.* **2015**, *332*, 127–137.
- (47) Qi, L.; Li, J. Z.; Wei, Y. X.; Xu, L.; Liu, Z. M. Role of naphthalene during the induction period of methanol conversion on HZSM-5 zeolite. *Catal. Sci. Technol.* **2016**, *6*, 3737–3744.
- (48) Chen, D.; Rebo, H. P.; Holmen, A. Diffusion and deactivation during methanol conversion over SAPO-34: a percolation approach. *Chem. Eng. Sci.* **1999**, *54*, 3465–3473.
- (49) Izadbakhsh, A.; Khorasheh, F. Simulation of activity loss of fixed bed catalytic reactor of MTO conversion using percolation theory. *Chem. Eng. Sci.* **2011**, *66*, 6199–6208.
- (50) Gao, M. B.; Li, H.; Yang, M.; Zhou, J. B.; Yuan, X. S.; Tian, P.; Ye, M.; Liu, Z. M. A modeling study on reaction and diffusion in MTO process over SAPO-34 zeolites. *Chem. Eng. J.* **2018**, DOI: 10.1016/j.cej.2018.08.054.
- (51) Li, Y. P.; Zhang, C. L.; Li, C. X.; Liu, Z. C.; Ge, W. Simulation of the effect of coke deposition on the diffusion of methane in zeolite ZSM-5. *Chem. Eng. J.* **2017**, *320*, 458–467.
- (52) Tian, G.; Wang, G.; Xu, C. M.; Gao, J. S. Gasification of the coke on spent-residue-pretreating catalysts with steam and steam–O<sub>2</sub> mixtures. *Energy Fuels* **2014**, *28*, 1372–1379.